

EFFICIENT AND ACCURATE TESTING OF AN EMC COMPLIANCE CHAMBER USING AN ULTRA WIDEBAND MEASUREMENT SYSTEM

Robert T. Johnk, David R. Novotny, and
Claude M. Weil
RF Technology Division
National Institute of Standards and Technology
NIST
325 Broadway
Boulder, Colorado 80303

Michael Taylor
Hach Company
Loveland, Colorado

Tony J. O'Hara
LARC TEC Marketing
Littleton, Colorado

Abstract

This paper summarizes a joint NIST-Industry measurement effort. The purpose of this effort was to use a NIST-developed ultrawideband measurement system to assess the performance improvement of ferrite tile anechoic chamber after a partial retrofit. Measurements were performed in the 30-1200 MHz frequency range before and after treatments were applied and excellent results were obtained. The system exhibited good sensitivity and the results highlight the effects of various retrofitting treatments. The effort also demonstrates that the NIST ultra wideband system is an efficient tool for the evaluation for both current and proposed anechoic EMC compliance test chambers.

Keywords: anechoic chamber, ferrite tile, figure of merit, performance metric, site attenuation, time-domain, ultrawideband, vector network analyzer

Introduction

The explosion of new consumer electronic devices has dramatically increased the workload of the EMC compliance testing community. There are increased demands to improve the accuracy and efficiency of emissions and immunity testing procedures. OATS sites are increasingly falling victim to RF pollution from Broadcast, Cellular and Industrial emissions. Semi-anechoic facilities are costly—due to the large volumetric requirements for height scanning over a ground plane. In response to this problem, CENELEC and the IEC [1] are exploring the use of fully anechoic rooms (FAR) with low-cost and efficient measurement capabilities. The ANSI C63 committee is forming a working group to formulate FAR compliance tests [2]. The evaluation of such facilities will require high-performance measurement systems while containing costs. NIST researchers and industry are evaluating the potential of a newly developed ultrawideband measurement system for the efficient examination of absorber-lined chambers.

*U.S. government work not subject to copyright

The NIST system provides significant advantages over the CW measurement systems specified in ANSI and CISPR standards:

- The NIST system eliminates the need for site-to-site comparisons—all of the necessary performance data is obtained from a set of chamber measurements
- The ability to directly observe the performance of the installed absorber system
- Eliminates the need for a separate quasi free-space reference by means of time gating, significantly reducing cost and time
- Much improved chamber diagnostic capability due to high range resolution capabilities
- Reduced chamber-antenna coupling

The NIST system was recently evaluated in a FAR room operated by a Colorado equipment manufacturer. The system was used to evaluate time-domain site attenuation, and the data was analyzed using two different chamber performance metrics. The system exhibited excellent measurement

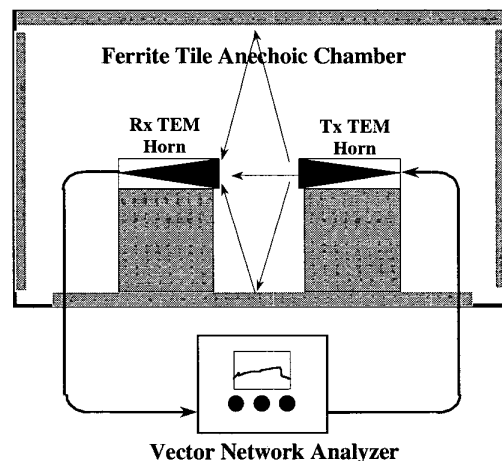


Figure 1. NIST ultrawideband chamber evaluation system

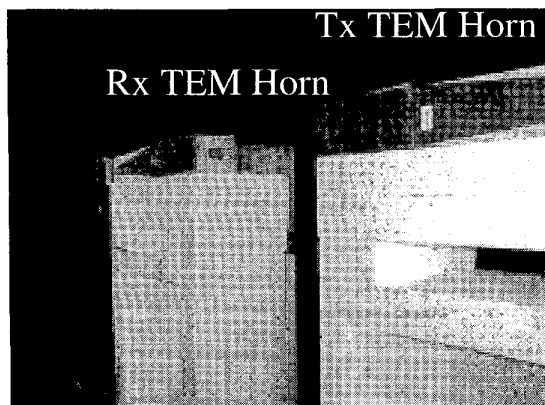


Figure 2. NIST measurement system inside a fully anechoic ferrite tile room. The transmitting and receiving horns are mounted on low-reflectivity styrofoam towers.

fidelity, and the results were used to recommend design changes. This system proved to be a good diagnostic tool and will provide valuable quantitative data on FAR facilities.

Measurement System

The measurement system used in this effort is shown in Figure 1, and consists of two TEM horns, a commercially available vector network analyzer, and precision 50 Ω interconnecting cables. The TEM horns are placed on low-reflectivity styrofoam towers at a fixed height and separation, as shown in Figure 2. CW transmission data (magnitude and phase) are obtained for each geometry over the frequency range of 2.4-2000 MHz. The data are then processed in a multiple-step signal processing sequence that permits the isolation of desired propagation events, resulting in the efficient evaluation of chamber performance. The two NIST-developed TEM horns provide excellent measurement fidelity and range resolution capabilities in the 25-1200 MHz frequency range. TEM horns are better suited for chamber evaluation than other EMC antenna types (e.g. biconical, log-periodic, hybrids) due to their short impulse-response characteristics. The NIST TEM horns have a relatively constant antenna factor from 30-1000 MHz, a characteristic not shared by traditional EMC antennas. The system acquires site attenuation magnitude and phase information in the frequency domain. The use of transmission measurements in conjunction with scalar EMI receivers and spectrum analyzers has been in use for many years as a chamber qualification tool [3]. The NIST measurement system provides a significant enhancement over current systems in that desired propagation events can be isolated and quantified. Measurement systems prescribed in current and proposed EMC standards do not have this unique capability [3,4]. This system has also been used to quantify the effects of an OATS shelter [5].

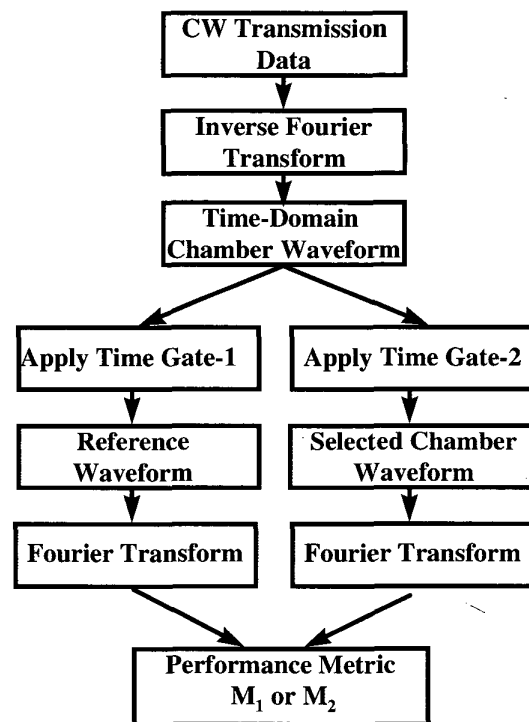


Figure 3. Signal processing sequence used to quantify chamber performance. Note that only one data set is required to generate a reference and quantify performance.

Signal Processing

The signal processing sequence used to isolate and quantify the desired propagation events is shown in Figure 3. The procedure can be summarized in four basic steps: **1.** Inverse Fourier transform CW magnitude and phase data to obtain a time-domain transmission record. **2.** Time gate the chamber record to isolate the direct antenna-to-antenna coupling waveform. **3.** Time gate the chamber record to isolate selected chamber propagation and scattering events. **4.** Fourier transform the time-gated waveforms of steps 2 and 3, and apply the results to a selected performance metric. The net result of this process is quantifying performance of this chamber over a selected frequency range.

The first step in this procedure is implemented by taking the frequency-domain S_{12} data obtained from the vector network analyzer and applying a Hanning window [6], followed by an Inverse Fast Fourier Transform (IFFT) to the time domain. The results of this process are depicted in Figure 4. The top waveform depicts a 20ns long segment of the chamber time-domain waveform obtained with this process for a 3m-antenna separation and a 1.2m height for both antenna heights. The first doublet on the waveform corresponds to the direct antenna-to-antenna coupling, which, in turn, is followed by the floor reflection and the ceiling/sidewall reflections. These events are localized in time and are amenable to time gating. By calculating the time of arrival of the various components,

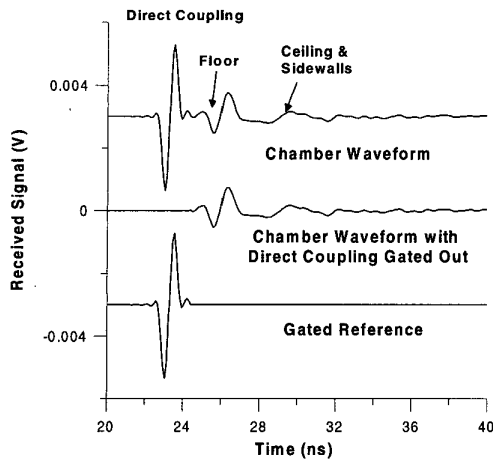


Figure 4. The top waveform is obtained from the Inverse Fourier transform of S_{12} data. The middle waveform is obtained by time-gating out the direct antenna-to-antenna coupling. The bottom waveform is the antenna-to-antenna coupling obtained by time gating.

the resulting waveform is easy to interpret and provides an excellent platform for understanding chamber physics, and establishes the foundation for an efficient time-frequency signal processing methodology.

Two time-gated waveforms are needed to assess the performance of a fully anechoic chamber: **1.** A time-gated reference waveform that effectively isolates the direct antenna-to-antenna coupling. **2.** A time-gated waveform that isolates desired chamber scattering—this may or may not include the direct coupling component. These waveforms are then Fourier transformed, and a division performed to obtain a frequency-dependent performance metric. Figure 5 depicts the resulting spectrum amplitudes obtained. The dashed line shows the spectrum amplitude of a time gated reference, corresponding to the direct antenna-to-antenna coupling. The use of a time-gated reference allows us to evaluate the chamber waveform without the necessity for a separate outdoor measurement setup, as is currently being proposed in the IEC and CENLEC [1] standards. The other curve includes chamber scattering, and the characteristics change dramatically—indicative of strong chamber reflections.

There are a number of ways in which a performance metric can be formed. One choice[7] is:

$$M_1 = \frac{|FT\{\text{entire chamber wfm}\}|}{|FT\{\text{gated ref wfm}\}|}, \quad (1)$$

Where FT denotes the Fourier transform. The performance metric M_1 is formed from the entire chamber waveform and a time-gated reference waveform that corresponds to the direct antenna-to-antenna coupling. The numerator in eq. (1) contains both the direct coupling and the scattering from the chamber. For a hypothetical perfect chamber in which there is no scattering from the chamber surfaces, the numerator of performance metric M_1 would contain only a direct-coupling

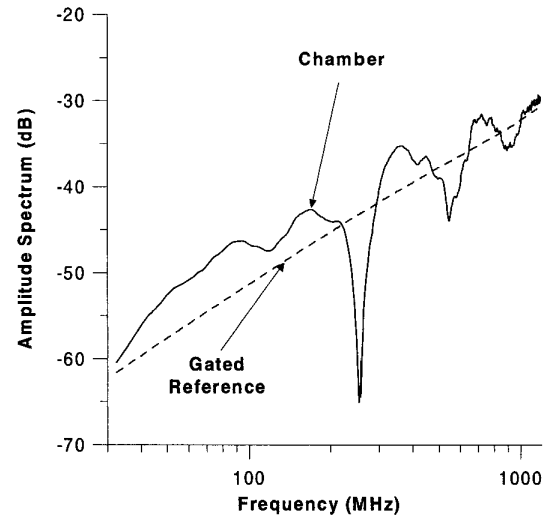


Figure 5. Fourier transformed spectrum amplitudes obtained from an entire chamber waveform and a time-gated reference. Note the dramatic differences due to strong chamber scattering effects.

term, and therefore would equal unity. This assumes, of course, that we neglect the contributions of internal antenna reflections and cable reflections, which are usually small in typical test setups. Deviations from unity (0 dB), therefore, represent imperfections in the chamber environment.

Another possible choice for a performance metric is given by:

$$M_2 = \frac{|FT\{\text{chamber wfm-gated ref wfm}\}|}{|FT\{\text{gated ref wfm}\}|}, \quad (2)$$

Where the direct antenna-to-antenna coupling is no longer included in the numerator. The performance metric M_2 provides a direct assessment of the chamber scattering and thereby the installed absorber system. A smaller value of M_2 indicates less scattering from the chamber environment and better performance. In fact, $M_2=0$ implies no scattering from the chamber environment and perfect behavior. The interference effects between the direct coupling and the chamber scattering are no longer present. As was shown in an earlier numerical study [7], this interference effect can cause M_1 to indicate good chamber performance when, in fact, the installed absorber system is performing quite poorly. The use of M_2 eliminates this problem and provides a much better indication of the behavior of the installed absorber system. The ability of the NIST system to differentiate between the direct antenna-to-antenna coupling and the chamber background is a capability unmatched by current, low-frequency EMC chamber evaluation systems.

Chamber Description and Enhancements

The facility in which the tests were performed is a compact, anechoic chamber with dimensions 3.65 m x 7.3 m x 3.65 m. The chamber is used for emissions and immunity measurements of both light and heavy industrial and laboratory instruments. The products measured are generally

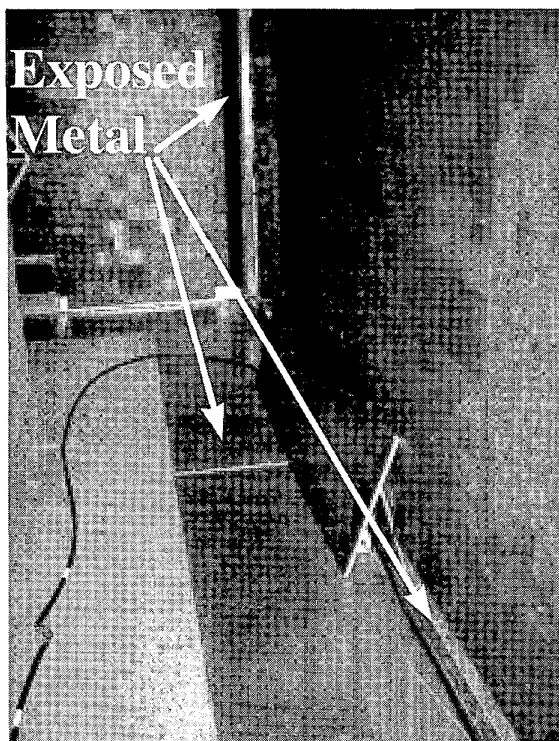


Figure 6. Exposed metal areas on the floor perimeter, base of the walls, and the door. Note the ESD carpet on the inner floor area.

less than 30 cm x 40 cm in size with fewer than 5 cables attached. The chamber has evolved over several years. It was originally constructed as a shielded room 8 years ago, in a compromise between compliance and production. To improve performance and reduce the uncertainties of measurements performed, ferrite tile absorber was installed 2 years later. Since that date, the process of continuous improvement has been ongoing.

The original chamber had bare metal walls. The first retrofit added ferrite tiles, completely covering the ceiling, and most of the side walls, except a 14 cm band left bare at the bottom of the walls. The floor was ferrite lined “throw-rug” style, with ferrite tiles in the center and a bare 40 cm area around the outside (see Figures 6 and 7). The floor tiles were covered with an ESD-safe carpet containing carbon-loaded threads to protect equipment under test. The original tile installation also left a 3.2 cm wide exposed metal band around the door. These exposed metal areas are shown in Figure 6. After extensive discussions and study by the authors, it was decided to cover the exposed areas around the door and the base of the wall. We will subsequently refer to this as a “stage-1” retrofit. Standing panels of ferrite tiles were constructed and placed in front of the waveguide air vents resting at approximately 35 degrees to the wall base. A similar panel was placed in front of the cable penetration panel at the base of the wall. Both of these panels are visible in Figure 6.

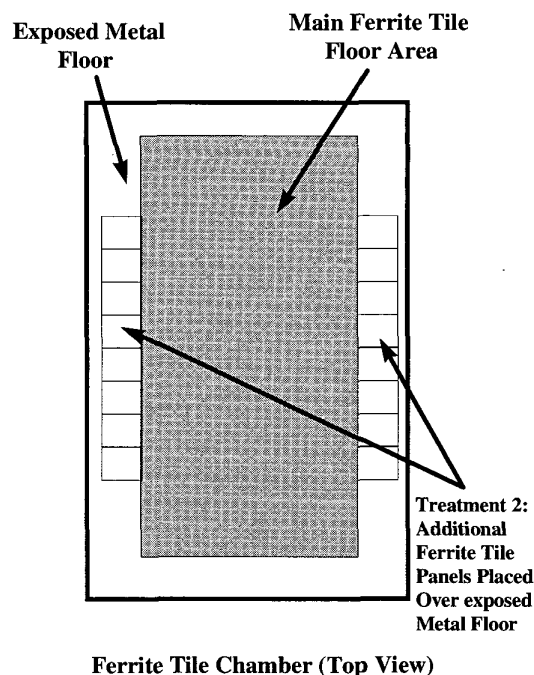


Figure 7. Stage 2 floor treatment. 2.4 m long sections of 30x30cm waffle tiles are added to the chamber floor perimeter.

These free standing panels subsequently had heavy gauge foil taped to the backside to improve low-frequency absorption. An additional “stage 2” enhancement was carried out and is shown in Figure 7. A 2.4 m length of waffled ferrite tile was added in the 40 cm gap on the floor midway from the EUT and the antenna of the floor. The authors felt that the exposed metal in the specular zone between the antennas might have a significant influence on the chamber performance.

Test Results

An extensive series of transmission measurements were performed in the chamber at three antenna-to-antenna separations and two different heights. All of the tests were carried out along the chamber centerline, since this is direction along which emissions and immunity tests are carried out. In order to evaluate the effects of the chamber enhancements, a baseline test was first conducted before the improvements, and then repeated after the stage-1 and stage-2 treatments. This methodology provides a differential basis of comparison and a high measurement sensitivity.

Figures 8 and 9 show results for the M_1 performance metric for which the antennas are symmetrically displaced with respect to the chamber center. For vertical polarization, an examination of Figure 8 shows a performance improvement with the stage 1 retrofit in the low-frequency range of 30-120 MHz. At the higher frequencies, the stage 1 retrofit has very little effect. With the addition of ferrite tiles in the metal gap

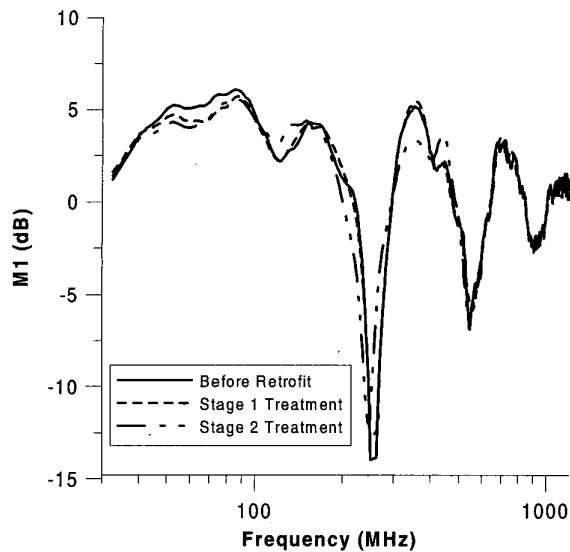


Figure 8. M_1 performance metric computed for vertical polarization, 3 m separation, and a 1.2 m height. Results are shown before and after stage 1 and 2 retrofits.

(stage 2), a performance improvement is extended up to 400 MHz. For horizontal polarization, the effects of the retrofits are quite different. Placing the ferrite tiles on the floor perimeter degrades the chamber performance from 100-500 MHz. This is probably due to the tuning effects of a mixed ferrite tile/metal boundary. The stage 1 retrofit now impacts the higher frequencies, and provides a noticeable performance improvement over the 250-450 MHz range. Degraded chamber performance is noted for both polarizations in the 200-300 MHz range, for which deviations in excess of 20 dB are noted with vertical polarization, and deviations in excess of 15 dB are seen in the horizontal case.

The reason for this will become apparent when we examine the M_2 performance metric results. The vertical and horizontal M_2 plots are shown in Figures 10 and 11. As was mentioned previously, The M_2 plots exclude the direct antenna-to-antenna coupling and contain the effects of the chamber scattering. High peak values of M_2 that have peak values of approximately 0 dB are observed in the 200-300 MHz range. In this case, the total chamber scattering is approximately equal to the direct antenna-to-antenna coupling, which accounts for the deep nulls observed in all of the M_1 plots—a result of interference between the direct coupling and chamber scattering. Another result of interest is the high values of chamber scattering below 100 MHz—a result indicative of poor low-frequency performance of the installed absorber system. As the frequency decreases below 100 MHz, the chamber scattering increases, due to the reduced performance of the ferrite tile absorber system. This result highlights a fallacy in using the M_1 performance metric, which shows better performance with decreasing frequency, due to direct/scattered wave interference. This is consistent with the findings of a numerical study conducted on ferrite tile chambers [7]. If one compares results above 100 MHz there

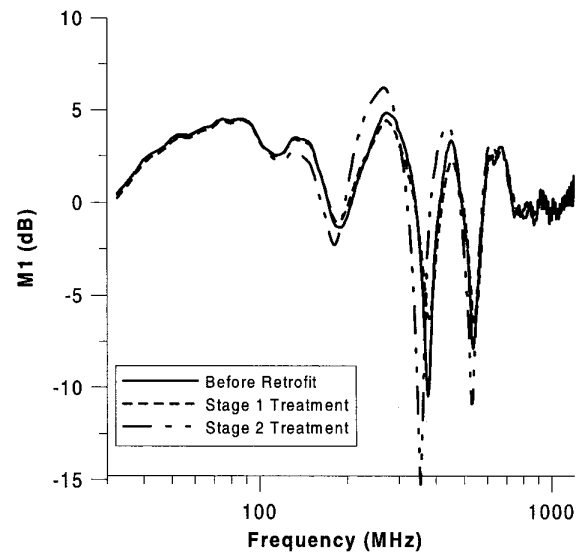


Figure 9. M_1 performance metric computed for horizontal polarization, 3 m separation, and a 1.2 m height. Results are shown before and after stage 1 and 2 retrofits.

is a consistent correlation between values of M_1 close to 0 dB and reduced values of M_2 . Conversely, there is a close correspondence between large deviations in M_1 and higher values of M_2 . Clearly, M_2 provides a more reliable indication of chamber performance.

The results indicate that performance improvements can be achieved by covering the exposed metal areas with additional ferrite tiles. Unfortunately the results are somewhat of a mixed bag, and the improvements are not global. Better performance is achieved at low frequencies with the stage 1 treatment with vertical polarization, but no real improvement is realized above 100 MHz. The situation reverses with horizontal polarization with improvements occurring above 200 MHz. The stage 2 treatment yields improved performance above 200 MHz with vertical polarization, but degrades with horizontal polarization. The results suggest that a more complete retrofitting process is required. One possibility that is currently being considered is to cover the remaining floor perimeter with ferrite tiles. Another, perhaps less attractive alternative is to totally remove the existing absorber system and replace it with a more optimized design. The current absorber system was purchased “off the shelf”, and it was not optimized for the room dimensions. Clearly, more modifications need to be performed on the chamber to correct the problems that occur in the 200-300 MHz frequency range. One effect that is observed in all of the data is a marked improvement in chamber performance above 800 MHz. This effect is due to the beam forming properties of the TEM horns at the higher frequencies where the antennas basically “talk” with each other and do not interrogate the chamber volume. This issue is currently being addressed by NIST researchers.

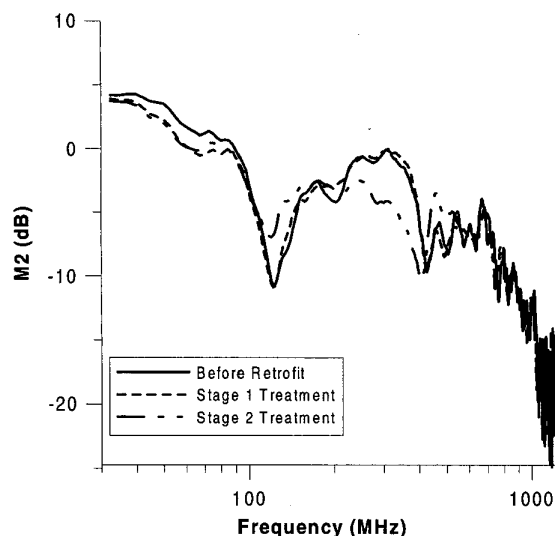


Figure 10. M_2 performance metric computed for vertical polarization, 3 m separation, and a 1.2 m height. Results are shown before and after stage 1 and 2 retrofits.

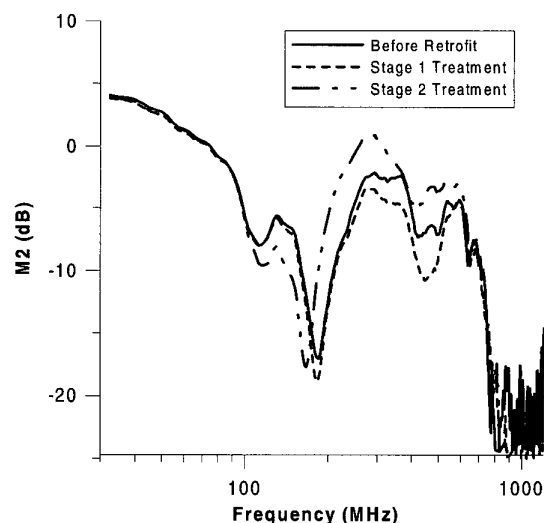


Figure 11. M_2 performance metric computed for horizontal polarization, 3 m separation, and a 1.2 m height. Results are shown before and after stage 1 and 2 retrofits.

Conclusions

An extensive measurement program was carried out in an industrial compliance test chamber before and after a two-stage retrofit. While the retrofitting process achieved performance improvements, consistent improvements were not achieved for both polarizations over the chamber frequency range of 30-1200 MHz. The results indicate that further improvements are needed, and these are currently being planned. The results of this effort demonstrates the power, fidelity, and efficiency of the NIST measurement system, as well as the distinct advantages that it possesses over conventional CW measurement systems. This is derived from an efficient time-frequency signal processing sequence that exploits the range resolution capabilities of an ultrawideband measurement system. The use of time gating permits the extraction of a reference from the chamber waveform and makes it unnecessary to perform a reference measurement in a quasi free-space environment, reducing the cost and time of chamber evaluations.

Acknowledgements

The authors are especially indebted to the Hach Company for its vision and support. We also thank Mr. David Seabury for his cooperation in providing the additional ferrite panels, and in sharing his extensive experience in optimization of anechoic chambers. Finally, we would like to thank Dr. Andy Repjar and Dr. Dennis Friday of the NIST (Boulder) RF Technology division for their vision and generous support.

References

- [1] CENELEC Draft prEN 50147-3, "Electromagnetic compatibility - basic emissions standard Part 3: emission measurements in fully anechoic rooms," European Committee for Electromechanical Standardization, Brussels, January, 2000.
- [2] ANSI C63 meeting, Redmond, WA, July 19-22, 2000.
- [3] ANSI C63.4-1988, American national standard methods of measurement of radio noise emissions from low-voltage electrical and electronic equipment in the range of 10 kHz to 1 GHz.
- [4] CISPR-16-1-10: 1999, Specifications for radio and immunity measuring apparatus and methods.
- [5] R.T. Johnk, D.R. Novotny, and C.M. Weil, "Assessing the effects of an OATS shelter: is ANSI C63.7 Enough?" Int. Symp. Digest on Electromagnetic Compatibility, Washington D.C., Aug. 20-25, 2000, Pp 523-528.
- [6] B. Gold and C. M. Rader, **Digital Processing of Signals**, McGraw Hill, New York, NY, 1969.
- [7] R. T. Johnk, D.R. Novotny, H.W. Medley, A.R. Ondrejka, C.L. Holloway, and P. McKenna, "Time-domain anechoic chamber site attenuation in low-frequency ferrite tile chambers," Proc. 21st Annual AMTA Symp., Monterey, CA, October 4-8, 1999.